Earthquake Related Deformation in Chile

This study focuses on the present-day deformation mechanisms of the south-central Chile margin. This plate tectonic margin has been the locus of several great subduction earthquakes in past centuries. The giant 1960 Valdivia event was the largest earthquake ever recorded instrumentally. ANSYS is used to understand and explain the present-day deformation of the Earth's surface that we observed with geodetic methods.

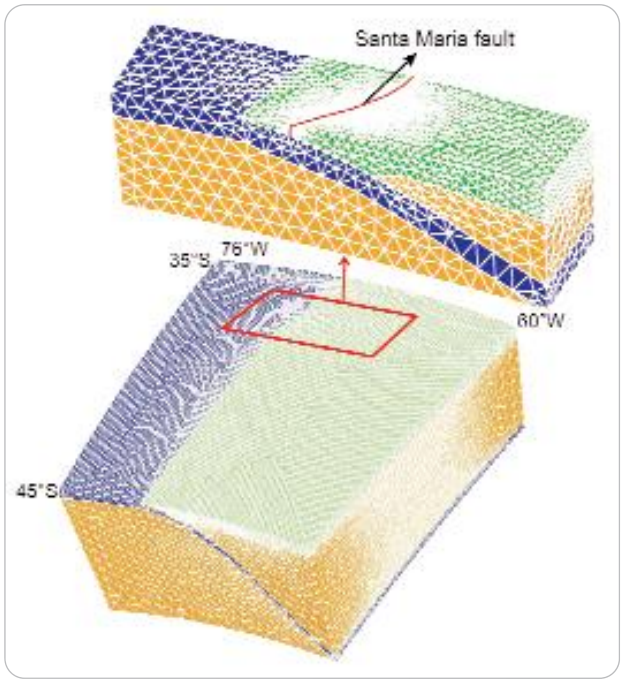

Fig. 1: 3-D finite element model setup. Green, blue and orange elements represent the continental and oceanic lithosphere and the mantle, respectively. Extracted portion of the mesh show details of the Santa Maria fault.

Contemporary deformation along active subduction margins primarily responds to the phases of the earthquake cycle [e.g., Thatcher and Rundle, 1979]. It is a transient and repetitive process conditioned by the mechanical coupling between the continental and oceanic plates. During the interseismic phase, high coupling between both plates results in the accumulation of contractional strain that is suddenly released as an earthquake. Coseismic rupture may be followed by aseismic slip and/or by prolonged postseismic deformation due to viscoelastic relaxation of the mantle.

The observed surface displacements were modeled with classical ANSYS 11.0. The spherical models are composed of 10-node tetrahedral-shaped elements and are constrained by kinematic boundary conditions. Element size is between 1 and 5 km in the fault zones and 10 km in the rest of the upper crust, whereas in the oceanic crust and mantle it is 10 and 50 km, respectively (Fig. 1). The models consist of an elastic upper plate, an elastic subducting plate, and a viscoelastic mantle. The mantle viscosity is initially set to 4×10^{19} Pa s. The observed deformation is modeled as:

1. Coseismic deformation (during the earthquake)

Elastic coseismic deformation is implemented using the split-node technique [Melosh and Raefsky, 1981]. It simulates the double-couple acting on the fault. Fig. 2 schematically shows the applied boundary conditions on the coseismic modeling. Each node on the contact faces is duplicated. Red and black nodes, which are part of the oceanic and continental plates, are initially located at the same coordinates. The seismogenic part of the interface is represented by the rupture and transition areas. In the rupture zone uniform coseismic slip is defined. This zone is surrounded by the transition zone that extends 10 km vertically below the rupture zone. The slip tapers linearly to zero also to the north and south of the rupture zone. Lateral transitions width is set to 50 km from the full slip zone. Outside of the transition zone, pair of nodes on the interface is coupled. We introduced the coseismic slip to each pair of nodes in the interplate using linear constraint equations. Nodes are forced to remain on the fault and consequently can only slide along the interface.

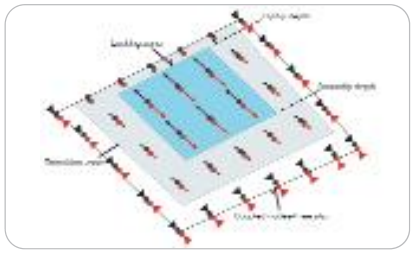

Fig. 2: Schematic illustration of the boundary condition applied on the fault plane. Red and black nodes belong to the oceanic and continental part of the interface, respectively. Arrows depict the constraints that simulate the double-couple acting on the fault.

2. Postseismic deformation (after the earthquake)

The coseismic slip changes the stress state of the subduction system suddenly and induces a postseismic response due to rheological properties of the lithosphere. During a megaearthquake the mantle resist the rapid elastic seaward motion of the forearc, accumulating large stress. This stress relaxes and decreases with time and may cause several decades of trench oriented deformation. A generalized Maxwell model is used to represent the viscoelastic material response of the Earth's mantle. The functions are represented in term of Prony series expansion for the shear and bulk modulus. Two primary factors influence the viscoelastic deformation over time: the coseismic slip distribution and the viscosity of the mantle. The viscosity directly controls the relaxation time and hence determines how fast the stress decays. To model the postseismic deformation we first applied an instantaneous load step solving the coseismic rupture. Next, the nodes on the interface are set free and a new load step is computed for time step T, which is equivalent to the period after the earthquake.

3. Interseismic Deformation (between the earthquakes)

Interseismic deformation is simulated using the back-slip method [Savage, 1983]. In this approach a virtual slip in a reverse sense to the plate motion is imposed on the fault interplate. The amount of plate convergence during one year (6.6 cm) is imposed as the backslip, using the vectors estimated from plate kinematics along strike of the plate interface. Next, we introduced the calculated vectors to each pair of nodes in the interpolated locked zone using linear constraint equations. The procedure is similar to the coseismic simulation.

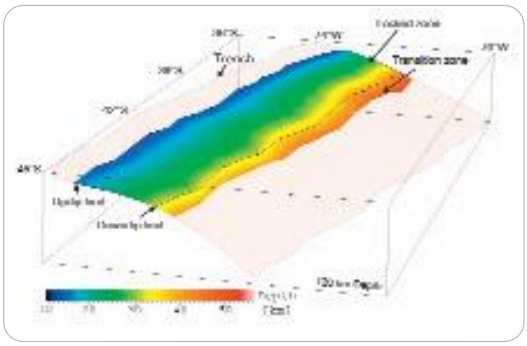

Fig. 3: Up- and downdip depth limits of the couple zone between 36°– 45° S. Below the downdip limit, a 10-km linear transition from fully-coupled to zero slip was applied

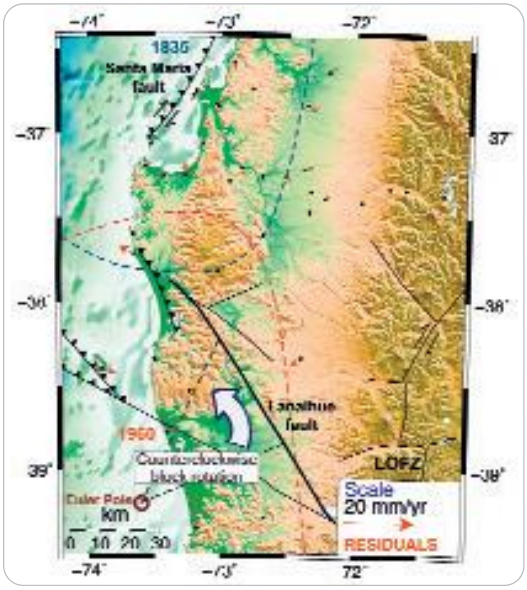

Fig. 4: Final residuals obtained by subtracting the modeled deformation (caused by interseismic and postseismic signals, effects of the Santa Maria fault, and rigid block rotation) from the observed deformation. Open circle at 39.2° S, 73.6° W show the Euler pole of rotation.

4. Crustal fault effect

An important part of our work is the introduction of the effect of crustal faults – namely the Santa Maria fault – on the interseismic model. The Santa Maria fault is modeled as a blind fault which extends from the interplate zone to a depth of 2 km (Fig. 2). The fault plane is introduced by contact-target surface elements. Following the split-node fault technique, we define the fault as two planes with identical distribution of nodes. Constraint equations are applied to introduce the slip rate on the fault. Contact-target elements obey the Coulomb friction criteria; surfaces can accumulate shear stresses up to a certain magnitude before they start sliding. The contact algorithms use the penalty stiffness method, with a contact option for closed gap, penetration reduction, exclusion of initial geometrical effect and no separation. Then, contact elements are prevented from penetrating the target surface but allow to slide along the fault.

Our modeling results show a wider coupled zone in the northern domain and a narrow zone in the south (Fig. 3). Postseismic model results infer mantle viscosities of 3.5×10^{19} Pa s. Expected patterns of vertical and horizontal deformation 45 years after the earthquake are well simulated. Residuals velocities obtained by subtracting the predicted interseismic and postseismic signals from the GPS velocities vectors have an average of 8 mm/yr. The Santa Maria fault model indicates a dextral strike-slip rate of 6.9 mm/yr, and a reverse dip slip rate of 2.8 mm/yr. The fault shows a friction coefficient of 0.6. Velocity residuals at the northern edge of the 1960 earthquake rupture zone can be explained by rigid block rotation (Fig. 4). We predict 5 – 7 mm/yr of lateral surface displacements across the Lanalhue fault.

Our study suggests that crustal-scale faults rooted in the interplate seismogenic zone may affect the surface deformation field during the earthquake cycle. We propose that these structures may release part of the contractional strain that accumulates during interseismic locking of the megathrust. Thus, active faults rooted in the plate interface should be considered when inverting geodetic data to constrain locking depths of the seismogenic zone. FEM plays a major role in our efforts to understand the nature of earthquakes and to estimate the related risk. <<

Authors

Marcos Moreno, Jürgen Klotz,
Helmholtz-Zentrum Potsdam, Germany,
Section 1.1 GPS/Galileo-Technology

References

Moreno, M., Klotz, J., Melnick, D., Echtler, H., Bataille, K. (2008) Active faulting and heterogeneous deformation across a megathrust segment boundary from GPS data, south-central Chile (36-39? S), Geochemistry Geophysics Geosystems, Vol. 9, No. 12.

Melosh, H. J., and A. Raefsky (1981), A simple and efficient method for introducing faults into finite element computations, Bull. Seismol. Soc. Am., 71 (5), 139121400.

Savage, J. (1983), A dislocation model of strain accumulation and release at a subduction zone, J. Geophys. Res., 88(B6), 4984?4996.

Thatcher, W. and J. Rundle (1979), A model for the earthquake cycle in underthrust zones., J. Geophys. Res., 84 (B10), 554025556.

Pictures

Helmholtz-Zentrum Potsdam, Germany

Information

www.gfz-potsdam.de